Development of an Engineering Diagram for Additively Manufactured Austenitic Stainless Steel Alloys

Zachary T. Hilton, Joseph W. Newkirk, Ronald J. O'Malley

Department of Materials Science and Engineering, Missouri University of Science and Technology, Rolla, MO 65409

Abstract

Austenitic stainless steels are the most widely applied types of stainless steels, due to their good weldability and high corrosion resistance. A number of engineering diagrams exist for the purpose of providing insight into the behavior of these steels. Examples of these diagrams are constitution diagrams (aka Schaeffler Diagrams) which are used to approximate the solidification path of the alloy and the amount of retained ferrite in the solidified matrix. Other diagrams are the Suutala diagram, which approximates cracking susceptibility, and microstructural maps, which predict the solidification path by varying a processing parameter, such as cooling rate. By combining these diagrams, a much more concrete conclusion can be made as to the behavior of a particular steel. This approach could be used to determine differences in behaviors between two different compositions. The developed diagram would be intended for use with rapid solidification phenomena as observed in the selective laser melting process.

Introduction

Constitution diagrams such as the Schaeffler diagram have long been used to predict the microstructural behavior of stainless steels in welding processes [1]. As welding technology has advanced, the cooling rates that can be achieved have increased, leading to inaccuracies in the predictions made with constitution diagrams. Figure 1 shows two compositions that the Schaeffler diagram predicts should have similar microstructural behaviors but, clearly, do not [1]. The Schaeffler diagram shown in Figure 2 predicts that compositions 1 and 2 should have the same FA solidification mode. Multiple attempts have been made to correct these diagrams and eliminate the inaccuracies; however, most attempts are limited by the available experimental data. The objective of the current study is to develop a diagram to better predict the behavior of stainless steel welds under high cooling rate conditions by combining published experimental data with thermodynamic simulations.
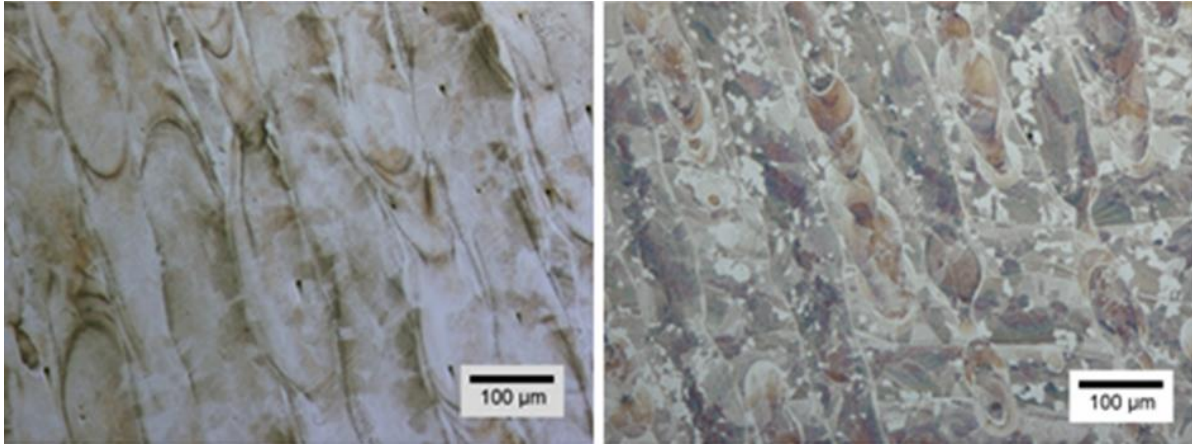
Figure 1. Micrographs of two compositions Schaeffler diagram predicts should have similar microstructures. Cr/Ni eq composition 1 is 1.51 and Cr/Ni eq composition 2 is 1.58. Samples clearly respond differently to the etching solution and reveal significantly different features. Left image from Reference 2. 60/40 nitric acid and water electrolytic etchant for 30 seconds.
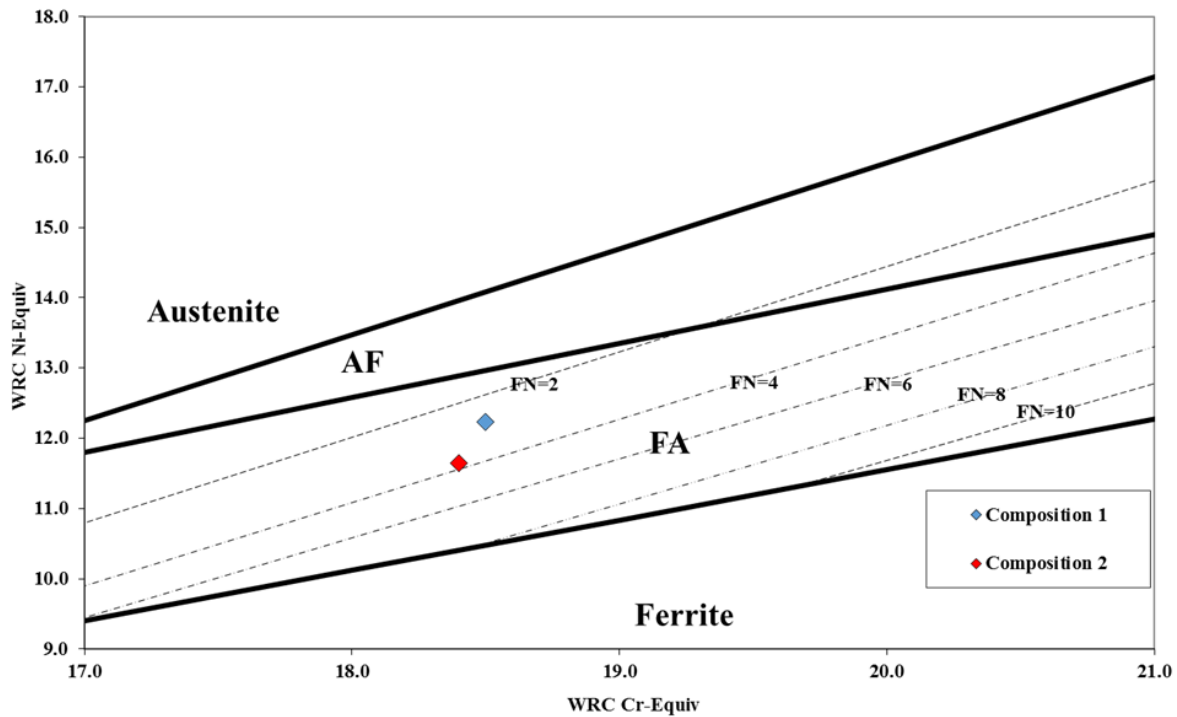

Figure 2. Schaeffler diagram with compositions 1 and 2, both predicted to have FA solidification mode.

Methodology

One of the more prominent attempts to develop a useful diagram is a microstructural map developed by Dr. John C. Lippold, shown in Figure 3, with compositions 1 and 2 plotted for reference [3]. Lippold developed this map as a first approximation based on the published data available at the time [3]. Upon reviewing the sources that Lippold used to develop the microstructural map, it is clear that the diagram could be improved to better fit the data [3-6]. Lippold used the assumption that, at low solidification rates, solidification should be dominated by the composition, not by solidification rate, and he uses this to justify having vertical boundary lines at the lower solidification rates. However, when the experimental data is plotted with the assumed line positions, the data shows a significant deviation from the assumed line positions.
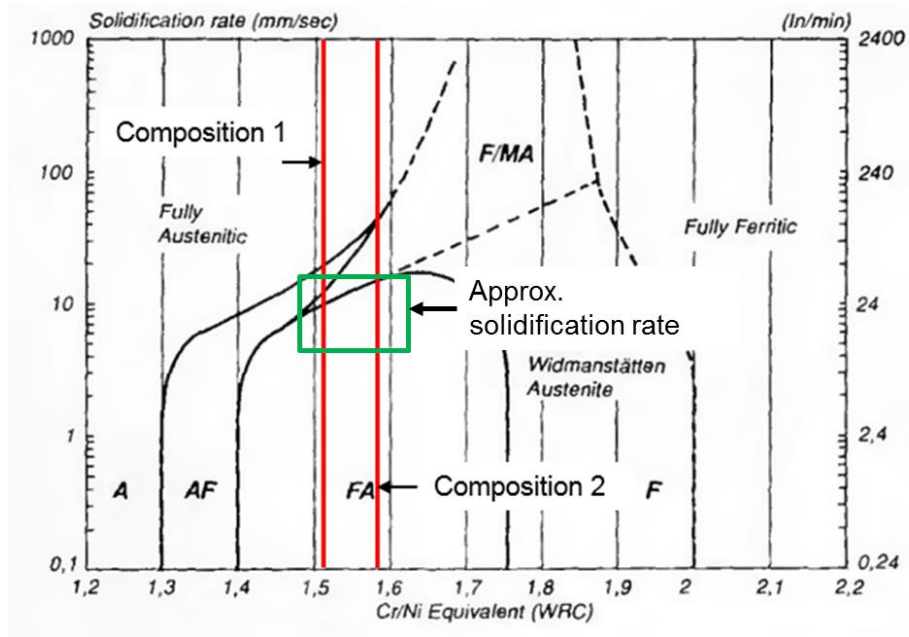

Figure 3. Microstructural map originally developed by Lippold [3]. Assumes weld microstructures not strongly dependent on solidification rate at lower solidification rates, indicated with vertical lines in those sections. Compositions 1 and 2 both predicted to have FA solidification mode.

The cited data sources for Lippold's microstructural map are papers written by Suutala, David et al, and a Ph.D. thesis by Elmer. Each of the three papers used a different method for calculating Cr and Ni equivalency values, but also reported their full chemistries, so all values were converted to match Lippold's method. The paper by Suutala summarizes its microstructural data with a table, and only considers three unique microstructures, labeled as austenitic-ferritic (AF), ferritic-austenitic (FA), and AF+FA, which is a combination of the previous two [4]. Suutala considered Cr/Ni values from 1.38 to 1.61 and welding speeds, which are assumed equivalent to solidification rates, from 0.416mm/sec to 13.33mm/sec. Using Suutala's data, it is clear that Lippold's microstructural map has a poor fit with the boundary between the AF and FA regions, and, as such, modifications can be made to better match Suutala's data [3-4]. David et al also summarized their data using a table and three unique phases. The phases used by David et al

are fully austenitic (A), austenitic and ferritic, and fully ferritic (F) [5]. These phase designations make it difficult to distinguish between the FA and AF regions, but provide a clearer picture of the transition points for the fully austenitic and fully ferritic regions. According to David et al's data, the boundary line between the A and AF regions could be altered to better represent the data, though the data is sparse in that region. The data from all the papers is also sparse in the regions above approximately 1.6 for Cr/Ni equivalency and approximately 30mm/sec [3-6]. Elmer's thesis provided additional points for this region [6]. Elmer's thesis also provided data as to the upper boundary of the AF and FA regions, though there is ambiguity in the exact values. The points shown in Figure 4, that are credited to Elmer's thesis, are the average of the possible range of values he presented [6]. Figure 4 demonstrates the fit between Lippold's microstructural map and the data from the three papers.
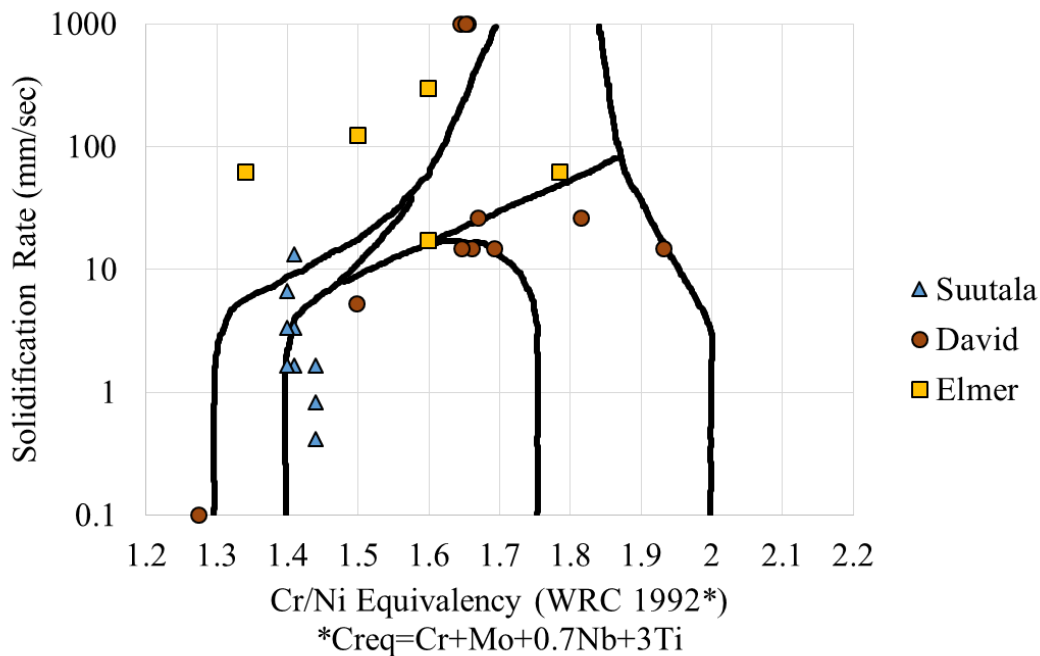

Figure 4. Lippold's microstructural map plotted with data. Map's fit has room for improvement. Data points presented taken from three source papers and converted to match dimensions of Lippold's map. Points attributed to Elmer are average values of ranges and are data points related to solidification mode transition boundaries. Elmer's data is plotted in this manner for clarity.

In the attempts to develop a more accurate microstructural map, the experimental data is often scattered and unevenly spaced, requiring interpolation to fill in any gray areas [4-6]. It is possible to reduce these gaps in the data through the use of predictive microstructural simulations. Such simulations are possible using the Dictra module of Thermo-Calc. In order to approximate different cooling rates, the user needs to modify the physical size of the system considered and set temperature as a function of time. The user can run solidification simulations that show when each new phase enters the system at any number of intermediate cooling rates and any desired composition.

Once the microstructural boundaries are more clearly defined and better understood, further modifications can be made to the microstructural map to allow for the prediction of regions at high risk for failure. Such a diagram was developed for use with Schaeffler diagrams and is shown in Figure 5. The areas of concern shown in the diagram in Figure 5 are hot cracking, martensitic cracking, and sigma phase embrittlement. Due to the suppression of martensite formation that is often observed in stainless steels, the region prone to failure will likely be small, if present at all [1]. Sigma phase is also unlikely to be a major concern during rapid solidification, as the material cools too rapidly for it to form during solidification [7]. The hot cracking region will likely be the most significant threat, as rapid cooling and more fully austenitic microstructures tend to promote its occurrence. A more accurate map may also allow for better in-process control of the microstructure as the cooling rate could be related back to the various building parameters.
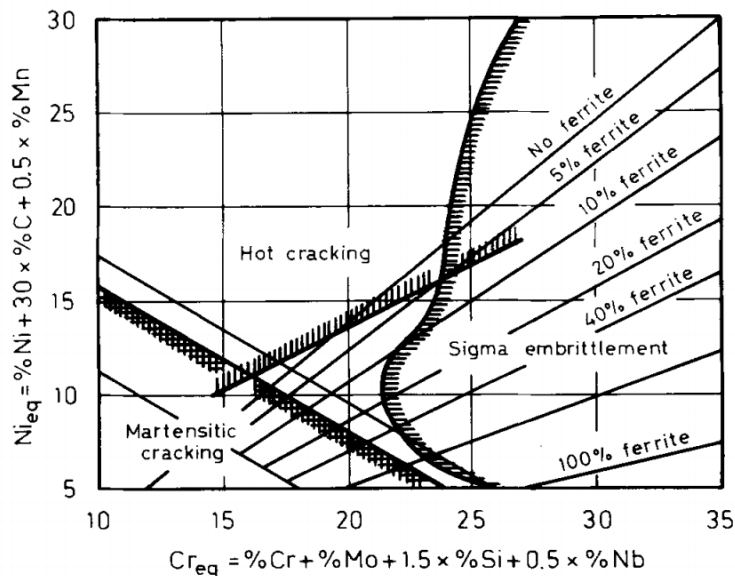

Figure 5. A modified Schaeffler diagram showing regions in which welds have a high risk of failure. Such regions could also be overlaid on a microstructural map, providing insight on their variation with solidification rate as well as composition [8].

Results and Discussion

As shown in Figure 4, significant improvement can be made to the fit of the microstructural map. The microstructural map predicted that both of the compositions presented in Figure 1 would most likely have microstructures that fell within the FA region. However, it appears that Composition 1 actually fell in the fully austenitic, or A, region due to the apparent microstructure. A map more accurate to both new and published data could provide a potential explanation for why the two compositions have different microstructural behavior. A key indicator of this difference is the response to the electrolytic nitric acid etchant. The etchant will preferentially attack ferrite over austenite. Composition 1 shows few signs of having been etched, while Composition 2 shows extensive signs of etching, indicating a difference in their solidified microstructures [6].

A more accurate microstructural map based on both the original data and the two compositions presented in this study, would still have weaknesses present in the diagram. The biggest issue is the lack of comprehensive data for the regions above 1.6 Cr/Ni equivalency and above a solidification rate of 30mm/sec. Elmer appears to be the most comprehensive source in that region, though that study only provides a limited number of data points for that region [6]. Another major weakness with the diagram is the approximate nature of its boundary lines [3]. In all the studies reviewed, there are several places where there is no data. For example, none of the studies presented any data for the microstructures present at compositions with a Cr/Ni equivalency between 1.79 and 1.91, despite the uncertainty as to the location of the fully ferritic transition [4-6]. The proposed simulations should be able to minimize these weaknesses, but would need to be confirmed with more comprehensive testing.

Conclusion

When used to predict the microstructure of rapidly solidified materials, constitution diagrams, such as the Schaeffler diagram, have been shown to be inaccurate. Several studies have attempted to develop diagrams to correct the inaccuracies of the Schaeffler diagram; one of the more prominent of which is the microstructural map developed by Lippold [3]. However, even these diagrams have weaknesses and could be improved in order to better predict the behavior of rapidly solidifying materials, such as additively manufactured stainless steels [3]. A review was conducted of the studies whose data Lippold used to develop the microstructural map and it was found that, according to that data, Lippold's map has a poor fit with the experimental data [4-6]. Lippold had assumed that a weld's microstructure was not strongly dependent on solidification rate at low solidification rates, which may have caused the diagram to poorly match the data used to create it [3]. As such, there is significant room for improvement of the microstructural map, which may be possible through the use of simulations. The simulations can be used to determine at what temperature each new phase enters the system, while varying the cooling rate and the composition. These simulations would allow for a much finer point distribution and, by extension, a potentially more accurate microstructural map, which could then be used to predict potential failure mechanism or to enable better in-process control of microstructure.

Acknowledgments

References

[1]   J. C. Lippold and D. J. Kotecki, *Welding Metallurgy and Weldability of Stainless Steels*. 2005.

[2]   T. Amine, C. S. Kriewall, and J. W. Newkirk, "Long-Term Effects of Temperature Exposure on SLM 304L Stainless Steel," *JOM*, vol. 70, no. 3, pp. 384–389, 2018.

[3]   J. C. Lippold, "Solidification Behavior and Cracking Susceptibility of Pulsed-Laser Welds in Austenitic Stainless Steels," *Weld. Res. Suppl.*, pp. 129–139, 1994.

[4]   N. Suutala, "Effect of Solidification Conditions on the Solidification Mode in Austenitic Stainless Steels," *Metall. Trans. A*, vol. 14, no. February, pp. 191–197, 1983.

[5]   S. A. David, J. M. Vitek, and T. L. Hebble, "Effect of Rapid Solidification on Stainless Steel Weld Metal Microstructures and its Implications on the Schaeffler Diagram," *Weld. J.*, no. October, pp. 289–300, 1987.

[6]   J. W. Elmer, "The Influence Of Cooling Rate On The Microstructure Of Stainless Steel Alloys by," Massachusetts Institute of Technology, 1988.

[7]   Z. T. Hilton, J. W. Newkirk, and R. J. O'Malley, "Studying Chromium and Nickel Equivalency to Identify Viable Additive Manufacturing Stainless Steel Chemistries," 2017.

[8]   N. Suutala, T. Takalo, and T. Moisio, "Ferritic-Austenitic Solidification Mode in Austenitic Stainless Steel Welds," *Metall. Trans. A*, vol. 11A, no. May, pp. 717–725, 1980.